The reliability and utility of on-site CT-derived fractional flow reserve (FFR) based on fluid structure interactions: comparison with FFR_{CT} based on computational fluid dynamics, invasive FFR, and resting full-cycle ratio

Yuto Fujii, MD[1]; Toshiro Kitagawa, MD, PhD[1]; Hiroki Ikenaga, MD, PhD[1]; Fuminari Tatsugami, MD, PhD[2]; Kazuo Awai, MD, PhD[2]; Yukiko Nakano, MD, PhD[1]

[1]Department of Cardiovascular Medicine, Hiroshima University Graduate School of Biomedical and Health Sciences, 1-2-3 Kasumi, Minami-ku, Hiroshima 734-8551, Japan

[2]Department of Diagnostic Radiology, Hiroshima University Graduate School of Biomedical and Health Sciences, 1-2-3 Kasumi, Minami-ku, Hiroshima 734-8551, Japan

Although not directly influencing the contents of this manuscript, co-author Kazuo Awai has a Collaborative Research Laboratory contract with Canon Medical Systems Corporation. All other authors declare no conflicts of interest associated with this manuscript.

***Correspondence:** Toshiro Kitagawa, MD, PhD

Department of Cardiovascular Medicine, Hiroshima University Graduate School of Biomedical and Health Sciences, 1-2-3 Kasumi, Minami-ku, Hiroshima 734-8551, Japan

Tel: +81-82-257-5540

Fax: +81-82-257-1569

Email: toshirok@hiroshima-u.ac.jp

Abstract

Background: Fractional flow reserve (FFR) derived off-site by coronary computed tomography angiography (CCTA) (FFR_{CT}) is obtained by applying the principles of computational fluid dynamics. This study aimed to validate the overall reliability of on-site CCTA-derived FFR based on fluid structure interactions (CT-FFR) and assess its clinical utility compared with FFR_{CT}, invasive FFR, and resting full-cycle ratio (RFR).

Methods: We calculated the CT-FFR for 924 coronary vessels in 308 patients who underwent CCTA for clinically suspected coronary artery disease. Of these patients, 35 patients with at least one obstructive stenosis (>50%) detected on CCTA underwent both CT-FFR and FFR_{CT} for further investigation. Furthermore, 24 and 20 patients underwent invasive FFR and RFR in addition to CT-FFR, respectively.

Results: The inter-observer correlation (r) of CT-FFR was 0.93 (95% confidence interval [CI] 0.85–0.97, P<0.0001) with a mean absolute difference of -0.0042 (limits of agreement -0.073, 0.064); 97.3% of coronary arteries without obstructive lesions on CCTA had negative results for ischemia on CT-FFR (>0.80). The correlation coefficient between CT-FFR and FFR_{CT} for 105 coronary vessels was 0.87 (95% CI 0.82–0.91, P<0.0001) with a mean absolute difference of -0.012 (limits of agreement -0.12, 0.10). CT-FFR correlated well with both invasive FFR (r=0.66, 95% CI 0.36–0.84, P=0.0003) and RFR (r=0.78, 95% CI 0.51–0.91, P<0.0001).

Conclusion: These data suggest that CT-FFR can potentially substitute for FFR_{CT} and correlates closely with invasive FFR and RFR with high reproducibility. Our findings should be proven by further clinical investigation in a larger cohort.

Keywords

Coronary computed tomography angiography

Fractional flow reserve

Fluid structure interaction

Computational fluid dynamics

Resting full-cycle ratio

Abbreviations

CAD coronary artery disease

CCTA coronary computed tomography angiography

CFD computational fluid dynamics

CT computed tomography

FFR fractional flow reserve

ICA invasive coronary angiography

iFR instantaneous wave-free ratio

RFR resting full-cycle ratio

Introduction

Determination of invasive fractional flow reserve (FFR) is the established method for assessment of the functional significance of coronary artery stenosis, and the prognosis of patients with coronary artery disease (CAD) is reportedly better when invasive FFR is used rather than invasive angiography to guide revascularization [1, 2]. Furthermore, the resting index, without the need for pharmacologic stress, such as the instantaneous wave-free ratio (iFR) or resting full-cycle ratio (RFR), has been applied in the clinical management of CAD. Recently, the principles of computational fluid dynamics (CFD) based on coronary computed tomography angiography (CCTA) images has been applied to estimate FFR, which is called as FFR_{CT} (HeartFlow Inc., Redwood City, CA, USA). Several multicenter studies have demonstrated that FFR_{CT} has incremental diagnostic value over CCTA [3-5]. Importantly, the 1-year outcomes in a large prospective registry study included less revascularization, a trend toward fewer major adverse cardiac events, and significantly fewer cardiovascular deaths or myocardial infarctions in patients with a negative FFR_{CT} result than in those with abnormal FFR_{CT} [6]. Therefore, this technique has potential benefit in the clinical setting of CAD.

The FFR_{CT} is typically calculated off-site via image transfer and is thus associated with delayed delivery of FFR_{CT} data to physicians. So far, an interaction network for communication of the original CCTA and FFR_{CT} data has generally been needed in Japan, which might prevent widespread clinical use of this parameter. The novel vendor-based technique for estimation of computed tomography (CT) -derived FFR, known as CT-FFR, offers a new option for clinicians [7, 8]. This technique employs fluid structure interaction by considering coronary shape, motility, cross-sectional area, and volume through CCTA data across the entire diastolic phase (70%–99%) of the cardiac cycle. It is based on a statistical estimation method for determination of patient-specific conditions for calculation of CT-FFR and can be performed on-site using a dedicated workstation.

A previous study has demonstrated the feasibility and high diagnostic accuracy of CT-FFR for assessment of the functional significance of coronary stenosis as determined by invasive FFR [9]. However, it failed to show a statistically significant difference when compared with anatomic CCTA findings for diagnosis of hemodynamically significant stenosis, possibly because of an underpowered sample size. Fujimoto et al analyzed the CT-FFR for 104 vessels with 30%–90% stenosis on CCTA and

found it to have excellent diagnostic accuracy for detection of a significant invasive FFR ≤0.80 and an iFR ≤0.89 compared with CCTA and to have high reproducibility [10].

To date, no head-to-head comparisons of FFR_{CT} and CT-FFR have been reported. In this study, we validated the overall reliability of CT-FFR analysis and compared CT-FFR data with FFR_{CT}, invasive FFR, and RFR data to assess the utility of CT-FFR in the clinical setting.

Methods

Study population

The target population in this retrospective study consisted of 326 patients who underwent CCTA at our institution between April 1, 2020 and November 9, 2022. CCTA was performed as the first detailed examination in patients who had coronary risk factors and warranted coronary artery evaluation, or who had chest symptoms and suspected angina pectoris, and as the further detailed examination in patients with suspected angina pectoris and positive exercise stress electrocardiogram or stress myocardial scintigraphy. In this study, to validate the reliability of CT-FFR measurements for overall assessment of coronary arteries, we applied CT-FFR analysis to all patients with visible vessel lumens of major epicardial coronary arteries on CCTA regardless of the CCTA findings; a subgroup with at least one 50%–90% stenosis in a major epicardial vessel >2 mm in diameter on CCTA and referred for further investigation underwent FFR_{CT} analysis as described below. Other subgroups of patients underwent invasive FFR and/or RFR for further assessment of the functional significance of coronary artery stenosis.

The exclusion criteria included renal insufficiency (estimated glomerular filtration rate <30 mL/min/1.73 m^2), asthma requiring long-term steroid therapy, history of previous revascularization procedures (PCI and/or CABG), and a contraindication to iodine-based contrast medium. The study protocol was approved by the Ethical Committee for Epidemiology of Hiroshima University (reference number E-2010). Informed consent was secured via the opt-out route in view of the non-interventional nature of the research and anonymity of the data.

CCTA acquisition

Patients with a pre-scan heart rate of ≥60 beats/min received oral metoprolol 20–40 mg and/or intravenous propranolol 2–10 mg. Patients in whom beta-blockers were contraindicated (due to severe aortic stenosis, systolic blood pressure <90 mmHg, history of asthma, symptomatic heart failure, or advanced atrioventricular block) did not receive these treatments. All patients received 0.6 mg of sublingual nitroglycerin. Patient preparation and CT scans were performed according to the Society of Cardiovascular Computed Tomography guidelines [11].

All patients underwent cardiac CT evaluation using a 320-row detector CT scanner (Aquilion ONE GENESIS Edition; Canon Medical Systems Corporation, Otawara, Japan). A non-contrast scan was performed to measure the coronary calcium score using the standard Agatston method (slice thickness 3.0 mm; maximum tube current 150 mA; tube voltage 120 kV) [12]. The dataset for CCTA was then acquired under a prospective ECG-gated single heartbeat scan with a phase window of 70%–99% of the R-R interval to cover the entire diastole (collimation 320 × 0.5 mm; tube current 750 mA; tube voltage 100–120 kV). Image reconstruction was performed using the Advanced intelligent Clear-IQ Engine (AiCE; Canon Medical Systems), which is an image reconstruction technique designed using deep learning.

The images were transferred to an AW workstation (GE Healthcare Japan Corporation, Tokyo, Japan), and evaluated for coronary lumen stenosis by two blinded observers working independently. The degree of stenosis was determined by obtaining the ratio of the lumen of the stenosis to the normal vessel diameter proximal or distal to the stenosis. The measurement was performed at an angle indicating the narrowest degree of stenosis using curved planar reconstructed images. Luminal stenosis >50% in any vessel was considered obstructive. Segments in which the coronary lumen could not be identified confidently due to severe calcification by either observer were excluded.

Regarding the definition of vessel characteristics, calcified plaque was defined as containing only a structure on the vessel wall with a CT density above that of the contrast-enhanced coronary lumen or with a CT density of >130 Hounsfield units (HU). Non-calcified plaque was defined as containing only a low-density mass >1 mm^2 in size, located within the vessel wall and clearly

distinguishable from the contrast-enhanced coronary lumen and the surrounding pericardial tissue. Partially calcified plaque was defined as containing both calcified plaque and non-calcified plaque components [13]. Positive remodeling was defined as coronary artery diameter at the plaque site >10% of the reference segment (positive remodeling index >1.1). Low attenuation plaque was defined as non-calcified plaque with internal attenuation <30 HU [14].

Calculation of CT-FFR

Dedicated algorithms based on fluid-structure interaction were used to calculate the patient-specific CT-FFR [7, 8]. In multiple volumes reconstructed from CCTA data at different time points during the diastolic wave-free period, the shape and changes in coronary vessel cross-sectional area were measured. Boundary conditions were derived using the following physical principles and relationships: 1) change in aortic volume is related to flow rate at the coronary artery inlet during diastole (70%–100%); 2) boundary pressure at the coronary artery outlet during diastole is related to cross-sectional lumen deformation, vessel stiffness, cross-sectional lumen shape, and the pressure at which the flow rate reaches zero; 3) the degree of loss of pressure between the aorta and the coronary artery outlet is related to the flow rate at the coronary artery outlet; 4) the resistance of microvascular vessels is minimized during diastole and constant such that pressure is proportional to flow [15]. The analytical conditions were determined using the Hierarchical Bayes method and Markov-Chain Monte Carlo method. Using these conditions and the Navier-Stokes equations, one-dimensional numerical fluid dynamics calculations were performed.

In this study, CT-FFR analysis was performed using a Vitrea workstation (Canon Medical Systems). CT data from 70% to 99% of the R-R interval were imported into the software [9], and the phase with the least movement was selected as the target phase. Next, the centerlines and contours of the three main coronary arteries were automatically calculated by the software. The user then reviewed the measurements and adjusted the centerlines and contours of the multiplanar and axial images for accurate lumen segmentation. After making the necessary edits, the contours of the remaining three volumes were automatically identified by the software, and the flow conditions were simulated using multiphase acquisition and fluid structure analysis. Finally, the CT-FFR values were

calculated for any given location on the coronary arteries. With regard to the measurement site of CT-FFR, it has been reported that when using invasive FFR in the distal segment as the reference standard, values measured 1-2 cm distal to the stenosis have shown significantly better diagnostic performance than values measured at far distal segments [16]. Therefore, in this study, CT-FFR values measured 1-2 cm distal to the stenosis were used for obstructive vessels. For non-obstructive vessels, values at the distal third were used. The time required for the analysis was defined as the interval between the start of analysis and acquisition of results using Vitrea workstation. To evaluate inter-observer variability in calculation of CT-FFR, two blinded operators working independently performed the calculations. CT-FFR was calculated at the same locations by the different operators using anatomical landmarks such as calcium deposits and side branches.

Calculation of FFR_{CT}

FFR_{CT} was derived by sending coronary CCTA data to HeartFlow Inc. using previously reported methods [17]. In brief, the coronary arteries and the proximal aorta were geometrically reconstructed as a three-dimensional model from the CCTA data. The overall coronary blood flow demand was then assessed by calculating the left ventricular myocardial volume, and the inflow and blood resistance during maximal aortic hyperemia were calculated as physiological conditions (all cases used fixed values for mean resting blood pressure, blood viscosity, and blood density). Blood flow and blood pressure under simulated maximal hyperemic conditions were calculated using patient-specific models. Next, using CFD, which quantified the pressure and velocity of fluids based on the laws of physics on a supercomputer, the flow and velocity at all points in the coronary arteries were analyzed using virtual blood flow, and FFR_{CT} at any given location on the coronary arteries was calculated. An $FFR_{CT} \leq 0.80$ was defined as positive for ischemia [3]. The FFR_{CT} values were measured 1-2 cm distal to the stenosis, at the same site where the CT-FFR values were measured. With regard to the measurement site of FFR_{CT}, it has also been reported that when using invasive FFR in the distal segment as the reference standard, values measured 1-2 cm distal to the stenosis have shown significantly better diagnostic performance than values measured at far distal segments [18], and the FFR_{CT} expert panel also recommended using FFR_{CT} values measured 1-2 cm distal to the stenosis [19].

The time required for the analysis was defined as the interval between the start of data transmission to HeartFlow Inc. and acquisition of results. Current FFR_{CT} technology has not been validated for calculating values <0.50. Therefore, a value of 0.50 was considered to indicate an occluded vessel or a vessel with an $FFR_{CT} \leq 0.50$.

ICA, FFR, and RFR

Invasive coronary angiography (ICA) was performed in at least two orthogonal directions for each evaluated coronary segment using a standard protocol. Before injection of contrast, 0.2 mL of nitroglycerin was administered via the intracoronary route for vasodilation of the epicardial coronary vessels. FFR was performed during ICA in at least one vessel with a diameter >2 mm and visible stenosis of 50%–90%. A 0.014-inch pressure guidewire (PressureWire X; Abbott Vascular, Santa Clara, CA, USA) was calibrated and electronically equalized with the aortic pressure before being placed in the distal segment of the evaluated coronary artery. Adenosine was injected intravenously at a rate of 140 μg/kg/min to induce maximal hyperemia of the coronary artery. FFR was calculated in the maximal hyperemic state by dividing the mean coronary artery pressure measured with a pressure sensor placed distal to the stenosis by the mean aortic pressure measured by the guiding catheter. Pressure wire pullback was then performed to check for pressure drift, and only runs with a pressure drift of ≤0.03 were accepted for analysis. Regarding the patients for whom RFR was also measured, it was measured in the resting state before intravenous injection of adenosine. To calculate RFR, the instantaneous coronary artery distal pressure (Pd) to aortic pressure (Pa) ratio (Pd/Pa) was measured automatically over five consecutive cardiac cycles. An FFR of ≤0.80 and an RFR of ≤0.89 were defined as functionally significant stenosis [1, 20]. All coronary angiography, FFR, and RFR data were acquired and interpreted by experienced blinded interventional cardiologists.

Statistical analysis

Continuous data are expressed as the mean ± standard deviation or as the median (interquartile range) as appropriate. Categorical data are expressed as the frequency (percentage). The correlation and agreement of CT-FFR with FFR_{CT}, invasive FFR, and RFR were evaluated using

Pearson's correlation coefficient and Bland-Altman analysis, as was inter-observer agreement. The optimal CT-FFR cutoff value for prediction of an invasive FFR ≤0.80 and an RFR ≤0.89 was determined by analysis of receiver-operating characteristic curves. All statistical analyses were performed using JMP 14.2 (SAS Institute Inc., Cary, NC, USA). A P-value of <0.05 was considered statistically significant.

Results

Baseline characteristics

CT-FFR analysis could not be performed for 18 of the 326 patients who underwent coronary CT because the coronary lumen was not completely visible in the sagittal view because of severe calcification. According to a general guideline for the proper use of FFR_{CT} in Japan, invasive coronary angiography was recommended for further examination in such patients. Of the remaining 308 patients in whom CT-FFR could be calculated, 35 with at least one 50%–90% stenosis in a major epicardial vessel >2 mm in diameter on CCTA underwent FFR_{CT} analysis. Invasive FFR was determined in 24 patients and the RFR in 20 patients in addition to CT-FFR (Figure 1). No patient was excluded from calculation of CT-FFR because of poor-quality CCTA images or from analysis of FFR_{CT} because of interference by severe imaging artifacts (e.g., noise, blooming, motion, misalignment) or because parts of the myocardium or coronary arteries were outside the field of view.

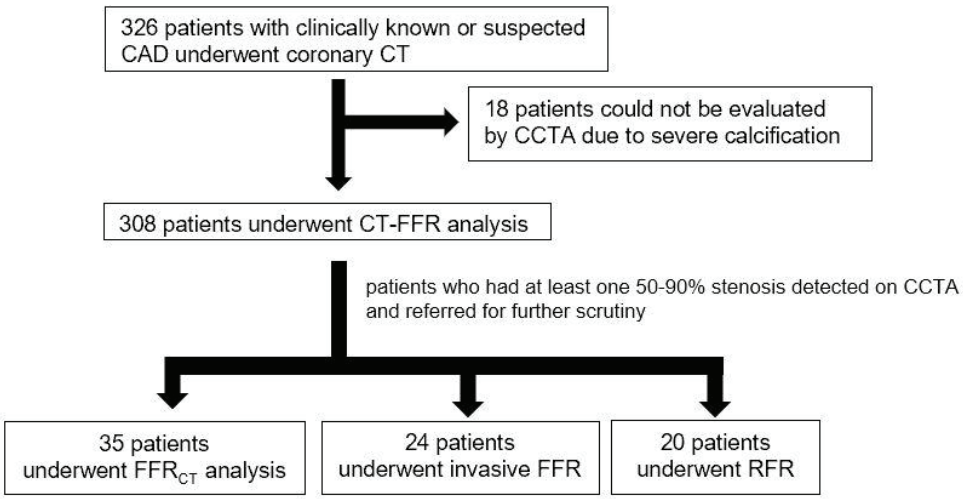

Fig. 1 Flow diagram showing the study enrollment process.

The patient and scan characteristics are shown in Table 1. Group comparisons were performed for patients who underwent further examination (FFR_{CT}, invasive FFR, RFR) and there were no significant differences.

Table 1. Baseline patient demographics and clinical characteristics

		Patients who underwent further investigation in addition to CT-FFR			P-value
	All patients who underwent CT-FFR (N=308)	FFR_{CT} (N=35)	invasive FFR (N=24)	RFR (N=20)	
Age (years)	67.0±10.9	72.7±7.0	69.4±8.5	67.9±8.5	0.071
Women	110(35.7%)	6(17.1%)	5(20.8%)	4(20.0%)	0.77
Body mass index	24.0±5.5	26.0±11.7	26.2±13.8	26.8±15.2	0.98
Hypertension	140(45.4%)	20(57.1%)	12(50.0%)	9(45.0%)	0.67
Dyslipidemia	105(34.1%)	10(28.6%)	8(33.3%)	8(40.0%)	0.69
Diabetes mellitus	43(14.0%)	7(20.0%)	7(29.2%)	6(30.0%)	0.62
Family history of coronary artery disease	88(28.6%)	11(31.4%)	8(33.3%)	7(35.0%)	0.96
Smoking					0.99
Former smokers	83(26.9%)	19(54.3%)	12(50.0%)	11(55.0%)	
Current smokers	43(14.0%)	3(8.6%)	3(12.5%)	2(10.0%)	
Never smoked	182(59.1%)	13(37.1%)	9(37.5%)	7(35.0%)	
Blood pressure prior to CCTA (mmHg)	138.4±21.9/ 78.5±14.0	141.1±22.2/ 79.6±17.0	138.3±23.9/ 75.3±12.4	135.9±22.8/ 75.4±10.5	0.71/0.42

Heart rate prior to CCTA (beats/min)	74.7±18.4	76.5±20.9	70.6±11.8	72.5±11.9	0.39
Pre-scan administration of beta-blockers					0.99
None	71(23.1%)	6(17.1%)	5(20.8%)	3(15.0%)	
Oral	68(22.1%)	8(22.9%)	6(25.0%)	5(25.0%)	
Intravenous	83(26.9%)	10(28.6%)	7(29.2%)	7(35.0%)	
Oral and intravenous	86(27.9%)	11(31.4%)	6(25.0%)	5(25.0%)	
Coronary calcium score	37(0-254)	388(49-860)	468(47-1168)	344(9-1271)	0.56

Data are expressed as the mean ± standard deviation (range), number (percentage) of patients, or median (interquartile range).

CT-FFR computed tomography-derived fractional flow reserve; FFR fractional flow reserve; FFR_{CT} fractional flow reserve derived off-site by coronary computed tomography angiography; *RFR* resting full-cycle ratio; *CCTA* coronary computed tomography angiography.

Reproducibility of CT-FFR and its diagnostic accuracy for assessing non-obstructive vessels

CT-FFR was calculated for 924 coronary arteries in 308 patients with an inter-observer correlation (r) of 0.93 (95% confidence interval [CI] 0.85–0.97, P<0.0001) and a mean absolute difference of -0.0042 (95% CI -0.019–0.011; limits of agreement, -0.073, 0.064).

In total, 787 of the 924 coronary vessels were deemed to having no obstructive lesions on CCTA; 766 vessels (97.3%) had a CT-FFR of >0.80. Of 21 vessels without obstructive lesions on CCTA and a CT-FFR of ≤0.80, 12 (57.1%) had myocardial bridging, 6 (28.6%) had moderate to severe calcification, and 3 (14.3%) had both. A representative case of a vessel with non-obstructive lesions on CCTA and a CT-FFR of ≤0.80 is shown in Figure 2.

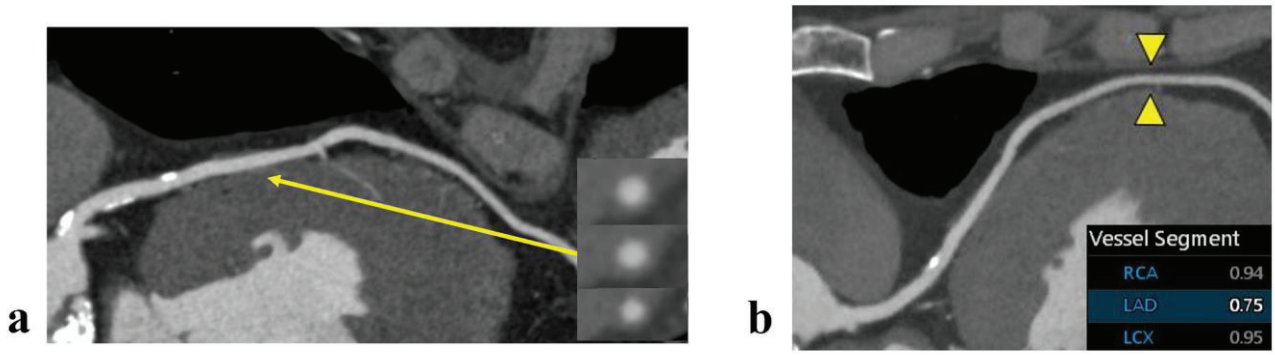

Fig. 2 Images for a 79-year-old man who presented with chest pains at night. Coronary computed tomography angiography demonstrated moderate calcification and slight myocardial bridging in the LAD, but there was no lesion with stenosis of greater than 50% (a). However, the computed tomography-derived fractional flow reserve was 0.75 in the LAD (b). *LAD* left anterior descending artery; *LCX* left circumflex artery; *RCA* right coronary artery.

CT-FFR versus FFR_{CT}

Both CT-FFR and FFR_{CT} were calculated for 105 vessels in 35 patients. We found a good correlation (r=0.87, 95% CI 0.82–0.91, P<0.0001; Figure 3A) and excellent agreement (mean difference -0.012; 95% CI -0.022– -0.001; limits of agreement -0.12, 0.10; Figure 3B) between CT-FFR and FFR_{CT}. In 64 vessels with obstructive lesions on CCTA, we found a similarly good correlation (r=0.88, 95% CI 0.81–0.93, P<0.0001; Figure 4A) and excellent agreement (mean difference -0.011; 95% CI -0.026–0.004; limits of agreement -0.13, 0.10; Figure 4B) between CT-FFR and FFR_{CT}. Table 2 shows the vessel based data for these lesions. When the cutoff value of CT-FFR was 0.80 as well as that of FFR_{CT}, the concordance rate of ischemia determination between CT-FFR and FFR_{CT} was 85.9% (55/64), and there were no significant differences in the cite of lesions, diameter stenosis, lesion length, classification of plaque morphology, frequency of positive remodeling, and frequency of low attenuation plaque between the concordance and non-concordance groups. Figure 5 shows representative cases in which CT-FFR and FFR_{CT} showed good agreement.

The average time for the analysis was shorter in CT-FFR than in FFR_{CT} (24.8 ± 4.3 min vs 157.0 ± 43.9 min, P<0.0001).

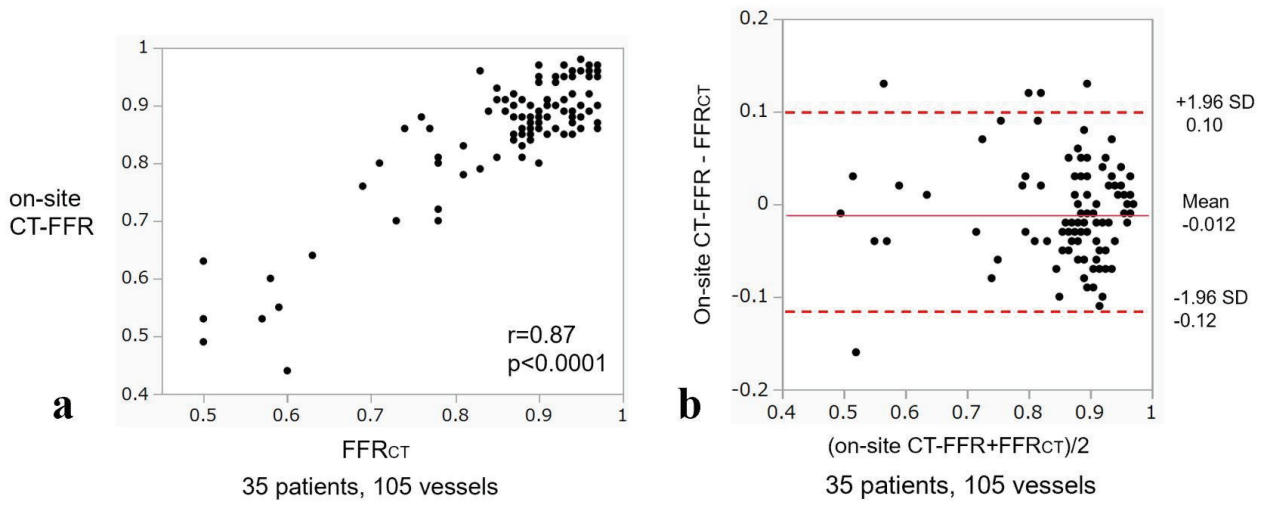

Fig. 3 (a) Correlation of CT-FFR and FFR_{CT} and (b) Bland–Altman plot of CT-FFR and FFR_{CT}. *CT-FFR* computed tomography-derived fractional flow reserve; *FFR_{CT}* fractional flow reserve derived off-site by coronary computed tomography angiography.

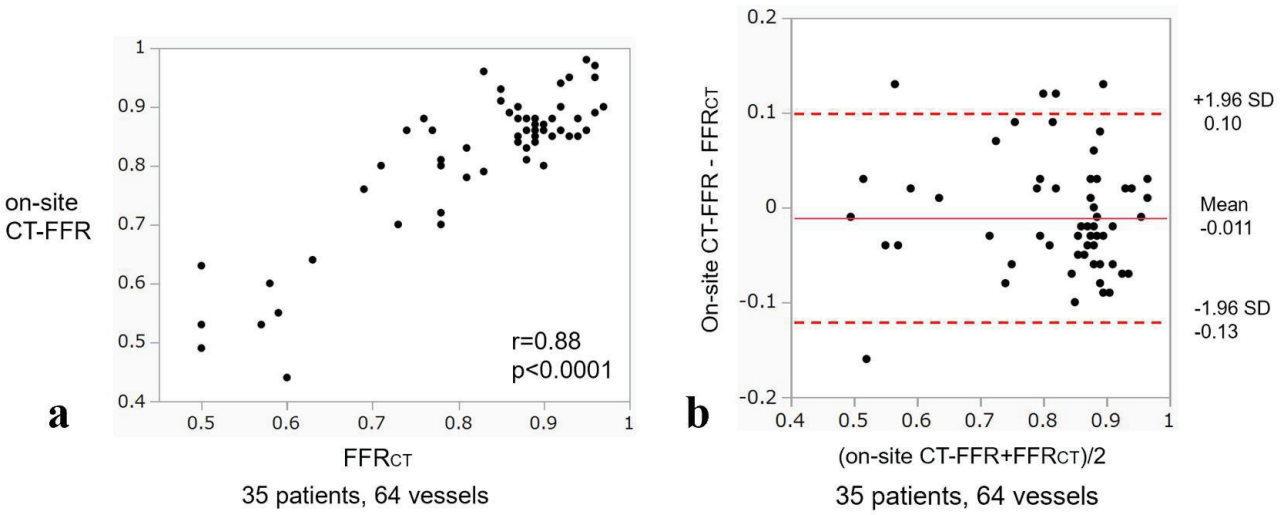

Fig. 4 (a) Correlation of CT-FFR and FFR_{CT} in vessels with stenotic lesions >50% on CCTA and (b) Bland–Altman plot of CT-FFR and FFR_{CT} in vessels with stenotic lesions >50% on CCTA. *CT-FFR* computed tomography-derived fractional flow reserve; *CCTA* coronary computed tomography angiography; *FFR_{CT}* fractional flow reserve derived off-site by coronary computed tomography angiography.

Table 2. Vessel based data on vessels that underwent FFR_{CT} in addition to CT-FFR

	All vessels (N=64)	Concordance between CT-FFR and FFR_{CT} (N=55)	Non-concordance between CT-FFR and FFR_{CT} (N=9)	P-value
RCA/LAD/LCX	17/34/13	15/28/12	2/6/1	0.65
diameter stenosis				0.44
50-70%	29 (45.3%)	26 (47.3%)	3 (33.3%)	
>70%	35 (54.7%)	29 (52.7%)	6 (66.7%)	
lesion length				0.33
<10mm	21 (32.8%)	20 (36.4%)	1 (11.1%)	
10-20mm	22 (34.4%)	18 (32.7%)	4 (44.4%)	
>20mm	21 (32.8%)	17 (30.9%)	4 (44.4%)	
classification of plaque morphology				0.90
Non-calcified plaque	18 (28.1%)	16 (29.1%)	2 (22.2%)	
Partially calcified plaque	25 (39.1%)	21 (38.2%)	4 (44.4%)	
Calcified plaque	21 (32.8%)	18 (32.7%)	3 (33.3%)	
positive remodeling	9 (14.1%)	7 (12.7%)	2 (22.2%)	0.45
low attenuation plaque	4 (6.3%)	4 (7.3%)	0 (0%)	0.40

Data are expressed as number (percentage) of vessels.

CT-FFR computed tomography-derived fractional flow reserve; *FFR_{CT}* fractional flow reserve derived off-site by coronary computed tomography angiography; *LAD* left anterior descending artery; *LCX* left circumflex artery; *RCA* right coronary artery; *RFR* resting full-cycle ratio

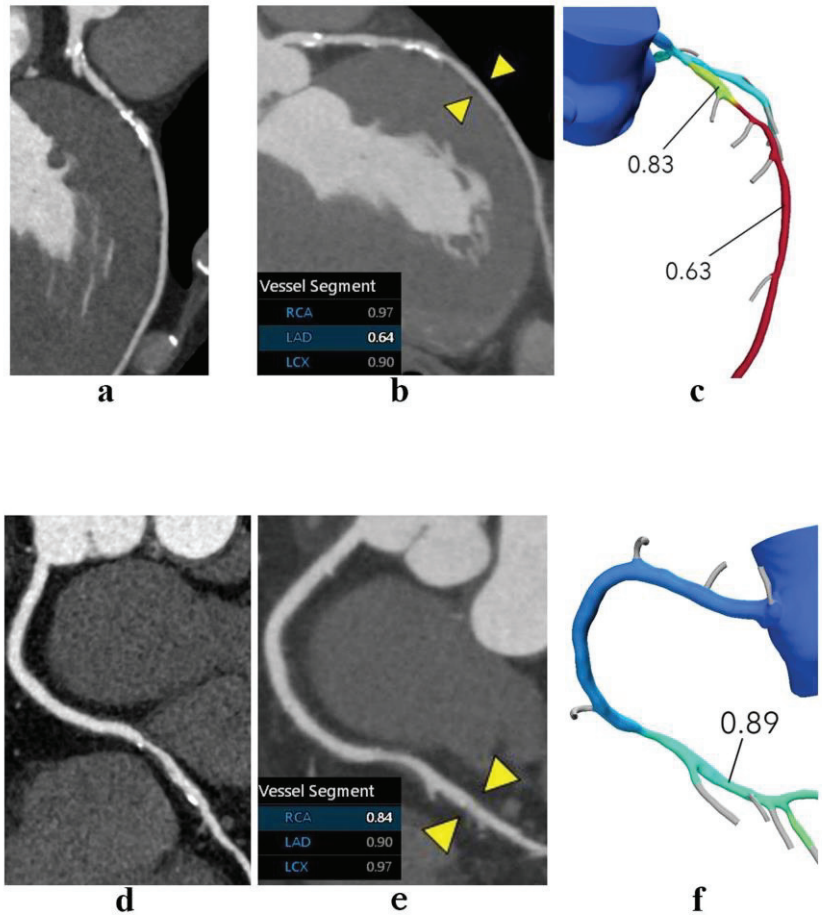

Fig. 5 (a-c) Images for a 76-year-old man with heart failure. Coronary computed tomography angiography demonstrated moderate stenosis with severe calcification in the LAD (a). The CT-FFR showed a positive result in the LAD (0.64) (b) and agreed with the result of FFR_{CT} (0.63) (c). (d-f) Images for a 78-year-old woman with dyspnea on exertion. Coronary computed tomography angiography demonstrated moderate stenosis in the RCA (d). The CT-FFR showed a negative value in the RCA (0.84) (e) and agreed with the result of FFR_{CT} (0.89) (f). *CT-FFR* computed tomography-derived fractional flow reserve; *FFR_{CT}* fractional flow reserve derived off-site by coronary computed tomography angiography; *LAD* left anterior descending artery; *LCX* left circumflex artery; *RCA* right coronary artery.

CT-FFR versus invasive FFR and RFR

Among the patients who underwent CT-FFR, invasive FFR was performed in 24 patients with 25 vessels and RFR in 20 patients with 20 vessels. In those patients, the correlation coefficient between CT-FFR and invasive FFR was 0.66 (95% CI 0.36–0.84, P=0.0003) and that between CT-FFR and RFR was 0.78 (95% CI 0.51–0.91, P<0.0001; Figure 6A, 6B). Figure 7A and 7B shows the receiver-operating characteristic curves for the ability of CT-FFR to predict an invasive FFR ≤0.80 and an RFR ≤0.89. The optimal CT-FFR cutoff value for prediction of an invasive FFR ≤0.80 was 0.75 (area under the curve, 0.79), which had a sensitivity of 81%, specificity of 78%, positive predictive value (PPV) of

87%, and negative predictive value (NPV) of 70%. The optimal CT-FFR cutoff value for prediction of an RFR ≤0.89 was 0.75 (area under the curve, 0.85), which had a sensitivity of 100%, specificity of 67%, PPV of 67%, and NPV of 100%. Figure 8 shows a representative case with positive results for ischemia on CT-FFR validated by invasive FFR and RFR. When the cutoff of CT-FFR was defined as 0.80, it had a sensitivity of 100%, specificity of 56%, PPV of 80%, and NPV of 100% for predicting an invasive FFR ≤0.80 and a sensitivity of 100%, specificity of 33%, PPV of 50%, and NPV of 100% for predicting an RFR ≤0.89.

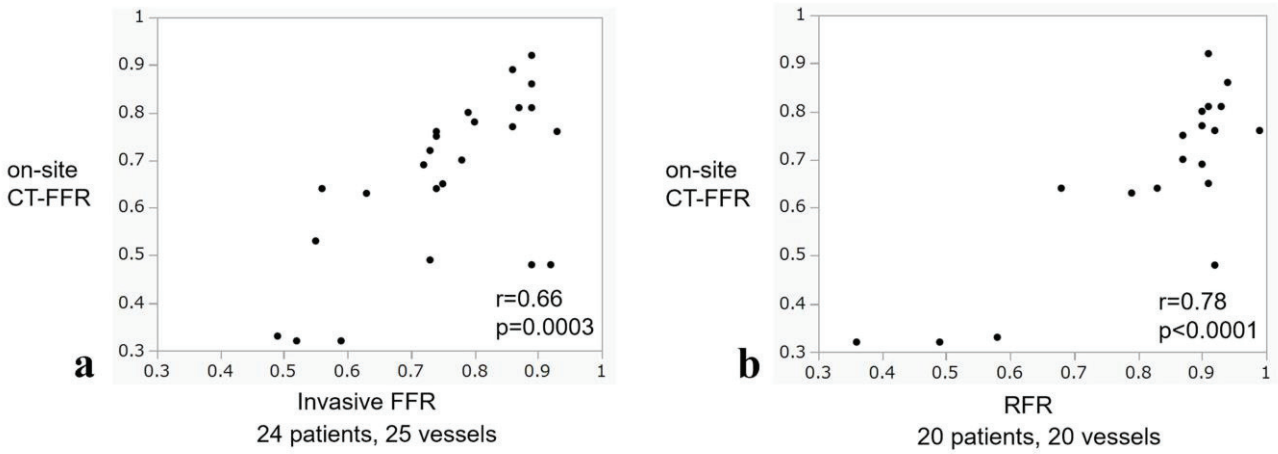

Fig. 6 (a) Correlation of CT-FFR and invasive FFR and (b) correlation of CT-FFR and RFR. *CT-FFR* computed tomography-derived fractional flow reserve; *FFR* fractional flow reserve; *RFR* resting full-cycle ratio.

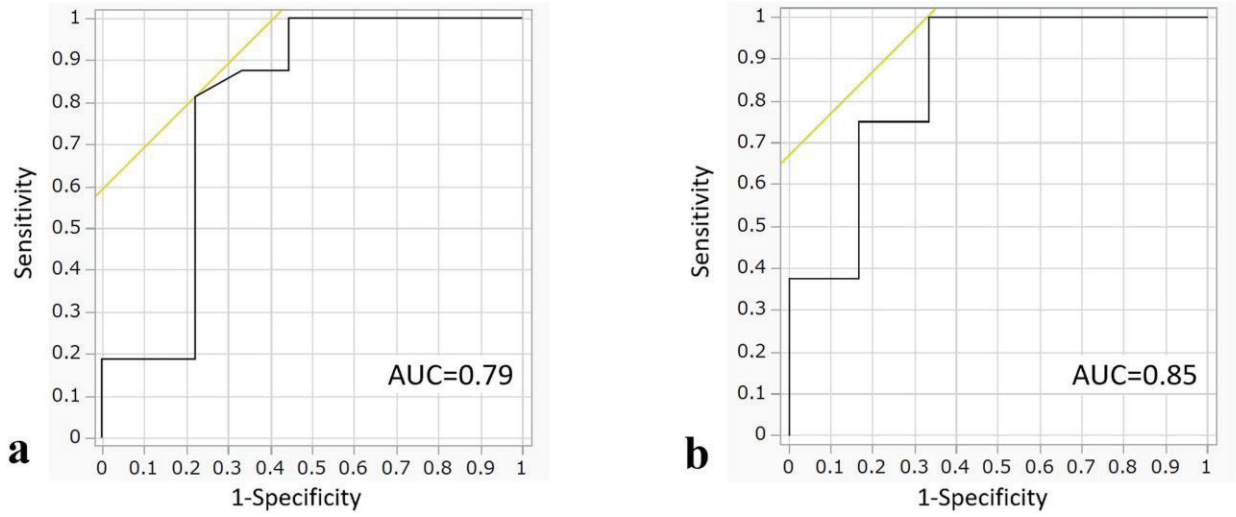

Fig. 7 (a) Area under the curve for prediction of invasive FFR ≤0.8 and (b) RFR ≤0.89. *AUC* area under the curve; *FFR* fractional flow reserve; *RFR* resting full-cycle ratio.

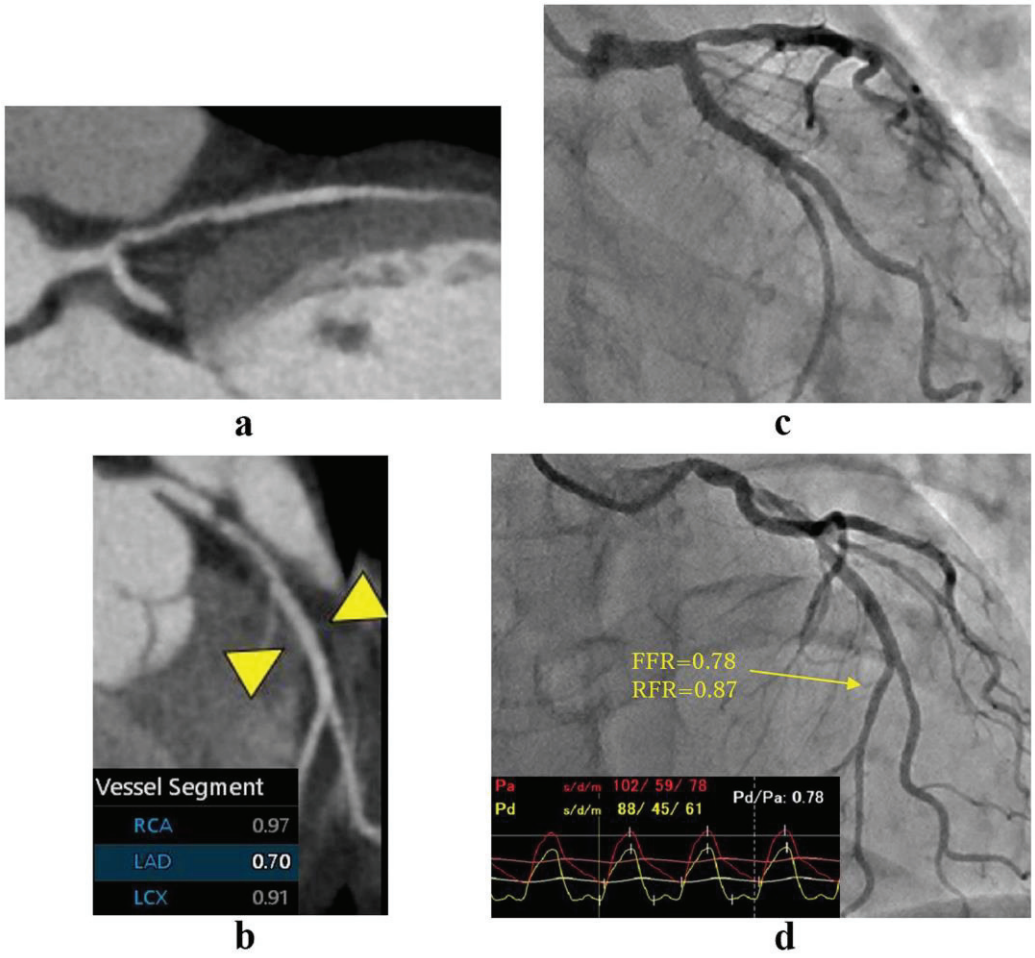

Fig. 8 Images for a 53-year-old woman with suspected exertional angina pectoris. Coronary computed tomography angiography demonstrated moderate stenosis in the proximal LAD (a). The CT-FFR result was positive (0.70) in the LAD (b). Invasive coronary angiography again demonstrated stenosis in the proximal LAD (c); both the FFR and RFR were positive (0.78 and 0.87, respectively) in the LAD (d). *CT-FFR* computed tomography-derived fractional flow reserve; *FFR* fractional flow reserve; *LAD* left anterior descending artery; *LCX* left circumflex artery; *RCA* right coronary artery; *RFR* resting full-cycle ratio.

Discussion

In this study, we investigated the reliability and utility of CT-FFR derived on-site in a clinical setting by retrospectively comparing CT-FFR data with FFR_{CT}, invasive FFR, and RFR data. Although there has been some research on the correlation between invasive FFR and FFR_{CT} and between invasive FFR and CT-FFR, to the best of our knowledge, this is the first study to examine the direct correlation between FFR_{CT} and CT-FFR data. We found the following: (1) CT-FFR had high

reproducibility based on interobserver agreement; (2) CT-FFR confirmed the absence of functionally significant stenosis when determined by CT-FFR >0.80 in nearly all coronary vessels without obstructive lesions on CCTA; (3) there was a good correlation and good agreement between CT-FFR and FFR_{CT}; and (4) there was a close correlation between CT-FFR and invasive parameters of coronary artery stenosis represented by FFR and RFR, indicating that CT-FFR has potential for noninvasive prediction of abnormalities in such parameters. Although the sample size is modest, our results provide significant evidence of the reliability and utility of CT-FFR in a clinical setting and demonstrate that this on-site modality has potential to substitute for the currently used FFR_{CT} with high reproducibility. Our findings may promote further application of CT-FFR in the management of CAD, which should be proved by further clinical investigation in a larger cohort.

CT-FFR enables patient-specific measurements to be obtained by direct analyses of patient data using a dedicated workstation on-site. As in previous studies [9, 10], we confirmed that CT-FFR has high inter-observer reproducibility, which highlights the clinical applicability of this technique. Furthermore, in this study, 97.3% of the vessels without >50% stenosis on CCTA were confirmed to be negative for ischemia on CT-FFR (determined by the cutoff of >0.80), suggesting that this method has high reliability for correct diagnosis of absence of functionally significant stenosis in the coronary arteries. However, we also found notable factors, namely, myocardial bridging and vessel calcification, which could be associated with overestimation of CT-FFR measurements. The squeezing phenomenon triggered by myocardial bridging may cause coronary blood flow reserve to be reduced not only during systole but also during part of diastole [21]. Given that CT-FFR is calculated in multiple cardiac phases during diastole, myocardial bridging could be the reason for 'false-positive' CT-FFR results. Blooming and beam-hardening artifacts derived from severe calcification blurred the vessel lumen in CCTA images, and 18 patients were excluded from calculation of CT-FFR because of severe calcification, as in a previous study [10]. Nevertheless, 42.9% (9/21) of the vessels without obstructive lesions on CCTA and a CT-FFR ≤0.80 had moderate to severe calcification. The relationship between the degree of coronary calcification and reliability of CT-FFR measurements should be further evaluated.

An important finding in this study was a direct correlation between FFR_{CT} and CT-FFR, which are calculated in different ways. FFR_{CT} is derived from hemodynamics calculated by CFD analysis, which is based on an anatomical and physiological model generated from CCTA data. CT-FFR is derived from fluid structure interaction analysis, in which CFD analysis is performed to calculate patient-specific boundary conditions using data for the four cardiac phases. Although CFD analysis is used in both, the processes used are different. When calculating FFR_{CT}, a patient-specific physiological model that represents aortic pressure and microcirculatory resistance at rest and at maximal hyperemia is created by calculating left ventricular myocardial volume and assessing overall coronary blood flow demand [17]. When calculating CT-FFR, patient-specific data on how the cross-sectional area of the coronary artery or the volume of the ascending aorta changes during the four cardiac phases are measured and utilized in the CFD analysis. Thus, both methods use patient-specific data, and a direct correlation between FFR_{CT} and CT-FFR was demonstrated in this study.

Unlike FFR_{CT}, CT-FFR enables on-site analysis, which is an advantage in daily clinical practice. FFR_{CT} requires time to send data for analysis by a supercomputer. Therefore, it is difficult to inform patients of the results on the same day of the examination because of the time required to receive the results. However, on-site analysis provides results in a short period of time, making it possible to inform patients of the results on the same day of the examination, even in a regular outpatient practice.

This study also shows that CT-FFR correlates closely with invasive intravascular parameters of coronary artery stenosis. Previous studies found a significant correlation between CT-FFR and invasive FFR with correlation coefficients of 0.57 and 0.52 [9, 10]. Although the sample size was smaller in this study, our correlation coefficient (0.66) was similar, and confirmed the accuracy of CT-FFR based on invasive FFR. Fujimoto et al. also demonstrated a significant correlation between CT-FFR and iFR with a correlation coefficient of 0.62 [10]. This study adds evidence of the accuracy of CT-FFR in comparison with another resting index, namely, RFR. RFR differs from iFR in that it is not only diastolic, but is also averaged over 5 heartbeats at the point of highest pressure gradient during the entire cardiac cycle. The RE-VALIDATE RFR trial, which prospectively compared the real-world diagnostic accuracy of RFR with that of iFR, found that RFR and iFR were equally accurate [22]. Our

study is the first to compare CT-FFR with a resting index other than iFR, and our finding of a significant correlation further supports the clinical accuracy and utility of CT-FFR. We also demonstrated that CT-FFR could predict invasive FFR ≤0.80 and RFR ≤0.89 fairly accurately; the optimal CT-FFR cutoff was 0.75 with a better specificity for both than a cutoff value of 0.80. The specificity of CT-FFR would be of value because CCTA has excellent sensitivity as an anatomical examination and also has good sensitivity of functionally significant stenosis. Thus, the CT-FFR cutoff 0.75 may be more useful in the clinical management of CAD.

Study limitations

Our study has several limitations. First, it had a single-center design and a small sample size, thus it is difficult to draw strong conclusions. Larger studies are needed to confirm our findings. Second, the study included patients with severe calcification and an Agatston score ≥400. It has been reported that the presence of calcified plaque has a significant effect on the diagnostic performance of CT-FFR [23], but the study also stated that it is independent of the degree of calcification indicated by the Agatston score. It is difficult to discuss in detail the influence of the degree and pattern of calcification on diagnostic performance of CT-FFR based on the present data. Third, current FFR_{CT} technology has not been validated for calculation of values <0.50. Therefore, a value of 0.50 was considered to indicate an occluded vessel or a vessel with an FFR_{CT} ≤0.50. Only three vessels had an FFR_{CT} of 0.50, which may have slightly influenced the correlation with CT-FFR. Fourth, 24 patients underwent both CT-FFR and invasive FFR, and 9 (10 vessels) were also analyzed by FFR_{CT}. Given the limited amount of data, it is difficult to discuss any correlation between these three measurement methods. As preliminary data, regarding the 10 vessels in which CT-FFR, FFR_{CT}, and invasive FFR were all performed, the accuracy of CT-FFR was 100% with no false positives or false negatives, while the accuracy of FFR_{CT} was 70% with 1 false positive lesion and 2 false negative lesions when using invasive FFR as the reference standard. Figure 9 shows a representative case in which the CT-FFR and FFR_{CT} ischemia determinations did not agree, and the CT-FFR result was confirmed by invasive

FFR. Further studies in more cases are needed to determine whether CT-FFR correlates better than FFR_{CT} with invasive FFR.

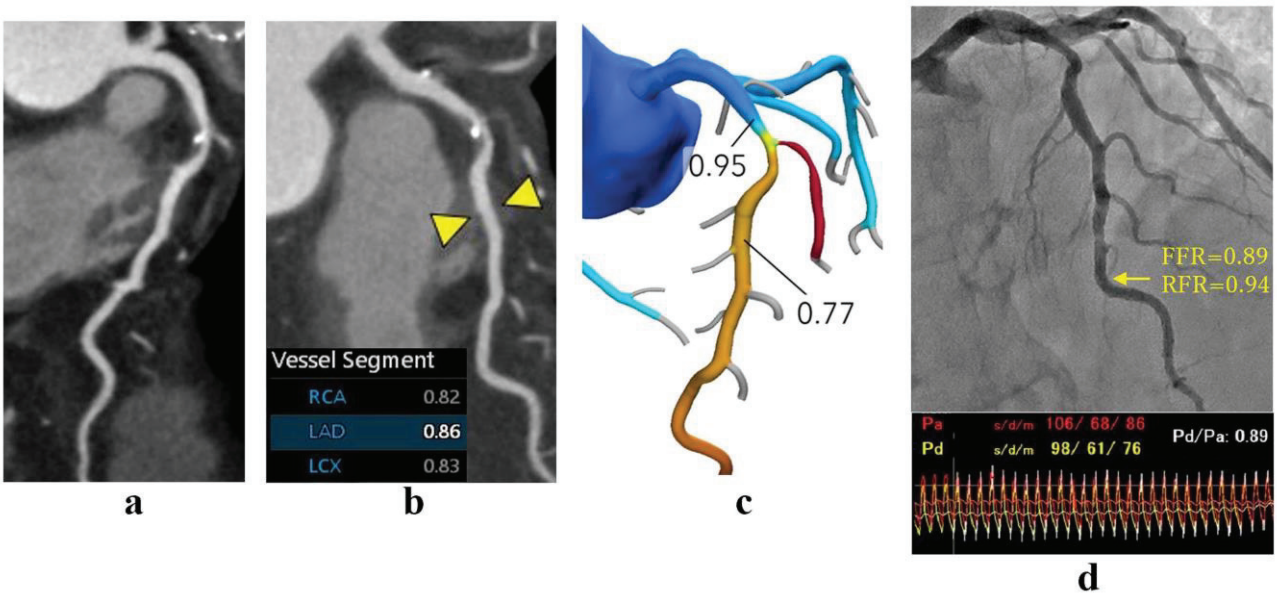

Fig. 9 Images for a 69-year-old man with intermediate risk of coronary artery disease. Coronary computed tomography angiography demonstrated moderate stenosis with moderate calcification in the LAD (A). The CT-FFR result was negative (0.86) in the LAD (B) and the FFR_{CT} result was positive (0.77) in the LAD (C). Invasive coronary angiography again demonstrated a stenosis in the LAD (D); the FFR and RFR results were both negative (0.89 and 0.94, respectively) in the LAD. *CT-FFR* computed tomography-derived fractional flow reserve; *FFR* fractional flow reserve; *FFR_{CT}* fractional flow reserve derived off-site by coronary computed tomography angiography; *LAD* left anterior descending artery; *LCX* left circumflex artery; *RCA* right coronary artery; *RFR* resting full-cycle ratio

Conclusions and clinical implications

CT-FFR may be useful as an on-site parameter that correlates significantly with FFR_{CT}, invasive FFR, and RFR with high reliability and reproducibility. Our findings should be proved by further clinical investigation in a larger cohort.

Acknowledgement

We thank Edanz (https://jp.edanz.com/ac) for editing a draft of this manuscript.

CRediT authorship contribution statement

Yuto Fujii: Conceptualization, Methodology, Formal analysis, Investigation, Data curation, Writing - original draft, Visualization. **Toshiro Kitagawa:** Conceptualization, Methodology, Writing - review & editing, Visualization. **Hiroki Ikenaga:** Investigation, Data curation. **Fuminari Tatsugami:** Investigation, Data curation. **Kazuo Awai:** Supervision. **Yukiko Nakano:** Supervision.

Funding

This research was supported by the Mochida Memorial Foundation for Medical and Pharmaceutical Research, and a JSPS KAKENHI Grant-in-Aid for Scientific Research (Grant Number 21K08127).

Declarations

Conflict of interest

Kazuo Awai has a Collaborative Research Laboratory contract with Canon Medical Systems Corporation. All other authors declare no conflicts of interest associated with this manuscript.

Ethical approval

Ethical approval for this study was given by the Ethical Committee for Epidemiology of Hiroshima University (reference number E-2010). Informed consent was secured via the opt-out route in view of the non-interventional nature of the research and anonymity of the data.

References

[1] Tonino PA, De Bruyne B, Pijls NH, Siebert U, Ikeno F, van' t Veer M, Klauss V, Manoharan G, Engstrøm T, Oldroyd KG, Ver Lee PN, MacCarthy PA, Fearon WF; FAME Study Investigators (2009) Fractional flow reserve versus angiography for guiding percutaneous coronary intervention. N Engl J Med 360:213-224.

[2] De Bruyne B, Fearon WF, Pijls NH, Barbato E, Tonino P, Piroth Z, Jagic N, Mobius-Winckler S, Rioufol G, Witt N, Kala P, MacCarthy P, Engström T, Oldroyd K, Mavromatis K, Manoharan G, Verlee P, Frobert O, Curzen N, Johnson JB, Limacher A, Nüesch E, Jüni P; FAME 2 Trial Investigators (2014) Fractional flow reserve-guided PCI for stable coronary artery disease. N Engl J Med 371:1208-1217.

[3] Koo BK, Erglis A, Doh JH, Daniels DV, Jegere S, Kim HS, Dunning A, DeFrance T, Lansky A, Leipsic J, Min JK (2011) Diagnosis of ischemia-causing coronary stenoses by noninvasive fractional flow reserve computed from coronary computed tomographic angiograms. Results from the prospective multicenter DISCOVER-FLOW (Diagnosis of Ischemia-Causing Stenoses Obtained Via Noninvasive Fractional Flow Reserve) study. J Am Coll Cardiol 58:1989-1997.

[4] Min JK, Leipsic J, Pencina MJ, Berman DS, Koo BK, van Mieghem C, Erglis A, Lin FY, Dunning AM, Apruzzese P, Budoff MJ, Cole JH, Jaffer FA, Leon MB, Malpeso J, Mancini GB, Park SJ, Schwartz RS, Shaw LJ, Mauri L (2012) Diagnostic accuracy of fractional flow reserve from anatomic CT angiography. JAMA 308:1237-1245.

[5] Nørgaard BL, Leipsic J, Gaur S, Seneviratne S, Ko BS, Ito H, Jensen JM, Mauri L, De Bruyne B, Bezerra H, Osawa K, Marwan M, Naber C, Erglis A, Park SJ, Christiansen EH, Kaltoft A, Lassen JF, Bøtker HE, Achenbach S; NXT Trial Study Group (2014) Diagnostic performance of noninvasive fractional flow reserve derived from coronary computed tomography angiography in suspected coronary artery disease: the NXT trial (Analysis of Coronary Blood Flow Using CT Angiography: Next Steps). J Am Coll Cardiol 63:1145-1155.

[6] Patel MR, Nørgaard BL, Fairbairn TA, Nieman K, Akasaka T, Berman DS, Raff GL, Hurwitz Koweek LM, Pontone G, Kawasaki T, Sand NPR, Jensen JM, Amano T, Poon M, Øvrehus KA, Sonck J, Rabbat MG, Mullen S, De Bruyne B, Rogers C, Matsuo H, Bax JJ, Leipsic J (2020) 1-Year

Impact on Medical Practice and Clinical Outcomes of FFR_{CT}: The ADVANCE Registry. JACC Cardiovasc Imaging 13:97-105.

[7] Hirohata K, Kano A, Goryu A, Ooga J, Hongo T, Higashi S, Fujisawa Y, Wakai S, Arakita K, Ikeda Y, Kaminaga S, Ko BS, Seneviratne SK (2015) A novel CT-FFR method for the coronary artery based on 4D-CT image analysis and structural and fluid analysis. SPIE Medical Imaging 2015 9412:652-666.

[8] Kato M, Hirohata K, Kano A, Higashi S, Goryu A, Hongo T, Kaminaga S, Fujisawa Y (2015) Fast CT-FFR analysis method for the coronary artery based on 4D-CT image analysis and structural and fluid analysis. In Proceedings of the American Society of Mechanical Engineers 2015 International Mechanical Engineering Congress and Exposition. ASME, New York, p.51124.

[9] Ko BS, Cameron JD, Munnur RK, Wong DTL, Fujisawa Y, Sakaguchi T, Hirohata K, Hislop-Jambrich J, Fujimoto S, Takamura K, Crossett M, Leung M, Kuganesan A, Malaiapan Y, Nasis A, Troupis J, Meredith IT, Seneviratne SK (2017) Noninvasive CT-Derived FFR based on structural and fluid analysis: A Comparison with invasive FFR for detection of functionally significant stenosis. JACC Cardiovasc Imaging 10:663-673.

[10] Fujimoto S, Kawasaki T, Kumamaru KK, Kawaguchi Y, Dohi T, Okonogi T, Ri K, Yamada S, Takamura K, Kato E, Kato Y, Hiki M, Okazaki S, Aoki S, Mitsouras D, Rybicki FJ, Daida H (2019) Diagnostic performance of on-site computed CT-fractional flow reserve based on fluid structure interactions: comparison with invasive fractional flow reserve and instantaneous wave-free ratio. Eur Heart J Cardiovasc Imaging 20:343-352.

[11] Abbara S, Blanke P, Maroules CD, Cheezum M, Choi AD, Han BK, Marwan M, Naoum C, Norgaard BL, Rubinshtein R, Schoenhagen P, Villines T, Leipsic J (2016) SCCT guidelines for the performance and acquisition of coronary computed tomographic angiography: a report of the society of Cardiovascular Computed Tomography Guidelines Committee: endorsed by the North American Society for Cardiovascular Imaging (NASCI). J Cardiovasc Comput Tomogr 10:435-449.

[12] Agatston AS, Janowitz WR, Hildner FJ, Zusmer NR, Viamonte M Jr, Detrano R (1990) Quantification of coronary artery calcium using ultrafast computed tomography. J Am Coll Cardiol 15:827-832.

[13] Kitagawa T, Yamamoto H, Toshimitsu S, Sasaki K, Senoo A, Kubo Y, Tatsugami F, Awai K, Hirokawa Y, Kihara Y (2017) ^{18}F-sodium fluoride positron emission tomography for molecular imaging of coronary atherosclerosis based on computed tomography analysis. Atherosclerosis 263:385-392.

[14] Cury RC, Abbara S, Achenbach S, Agatston A, Berman DS, Budoff MJ, Dill KE, Jacobs JE, Maroules CD, Rubin GD, Rybicki FJ, Schoepf UJ, Shaw LJ, Stillman AE, White CS, Woodard PK, Leipsic JA (2016) CAD-RADS(TM) Coronary Artery Disease - Reporting and Data System. An expert consensus document of the Society of Cardiovascular Computed Tomography (SCCT), the American College of Radiology (ACR) and the North American Society for Cardiovascular Imaging (NASCI). Endorsed by the American College of Cardiology. J Cardiovasc Comput Tomogr 10(4):269-281.

[15] Sen S, Escaned J, Malik IS, Mikhail GW, Foale RA, Mila R, Tarkin J, Petraco R, Broyd C, Jabbour R, Sethi A, Baker CS, Bellamy M, Al-Bustami M, Hackett D, Khan M, Lefroy D, Parker KH, Hughes AD, Francis DP, Di Mario C, Mayet J, Davies JE (2012) Development and validation of a new adenosine-independent index of stenosis severity from coronary wave intensity analysis: results of the ADVISE (ADenosine Vasodilator Independent Stenosis Evaluation) study. J Am Coll Cardiol 59:1392-1402.

[16] Nozaki YO, Fujimoto S, Aoshima C, Kamo Y, Kawaguchi YO, Takamura K, Kudo A, Takahashi D, Hiki M, Kato Y, Okai I, Dohi T, Okazaki S, Tomizawa N, Kumamaru KK, Aoki S, Minamino T (2021) Comparison of diagnostic performance in on-site based CT-derived fractional flow reserve measurements. Int J Cardiol Heart Vasc 35:100815.

[17] Taylor CA, Fonte TA, Min JK (2013) Computational fluid dynamics applied to cardiac computed tomography for noninvasive quantification of fractional flow reserve: scientific basis. J Am Coll Cardiol 61:2233-2241.

[18] Omori H, Hara M, Sobue Y, Kawase Y, Mizukami T, Tanigaki T, Hirata T, Ota H, Okubo M, Hirakawa A, Suzuki T, Kondo T, Leipsic J, Nørgaard BL, Matsuo H (2021) Determination of the Optimal Measurement Point for Fractional Flow Reserve Derived From CTA Using Pressure Wire Assessment as Reference. AJR Am J Roentgenol 216(6):1492-1499.

[19] Norgaard BL, Fairbairn TA, Safian RD, Rabbat MG, Ko B, Jensen JM, Nieman K, Chinnaiyan KM, Sand NP, Matsuo H, Leipsic J, Raff G (2019) Coronary CT angiography-derived fractional flow reserve testing in patients with stable coronary artery disease: recommendations on interpretation and reporting. Radiol Cardiothorac Imaging 1(5):e190050.

[20] Lee JM, Choi KH, Park J, Hwang D, Rhee TM, Kim J, Park J, Kim HY, Jung HW, Cho YK, Yoon HJ, Song YB, Hahn JY, Nam CW, Shin ES, Doh JH, Hur SH, Koo BK (2019) Physiological and Clinical Assessment of Resting Physiological Indexes. Resting Full-Cycle Ratio, Diastolic Pressure Ratio, and Instantaneous Wave-Free Ratio. Circulation 139:889-900.

[21] Ge J, Erbel R, Rupprecht HJ, Koch L, Kearney P, Görge G, Haude M, Meyer J (1994) Comparison of intravascular ultrasound and angiography in the assessment of myocardial bridging. Circulation 89:1725-1732.

[22] Kumar G, Desai R, Gore A, Rahim H, Maehara A, Matsumura M, Kirtane A, Jeremias A, Ali Z (2020) Real world validation of the nonhyperemic index of coronary artery stenosis severity - Resting full-cycle ratio - RE-VALIDATE. Catheter Cardiovasc Interv 96(1):E53-E58.

[23] Kawaguchi YO, Fujimoto S, Kumamaru KK, Kato E, Dohi T, Takamura K, Aoshima C, Kamo Y, Kato Y, Hiki M, Okai I, Okazaki S, Aoki S, Daida H (2019) The predictive factors affecting false positive in on-site operated CT-fractional flow reserve based on fluid and structural interaction. Int J Cardiol Heart Vasc 23:100372.